JERZY MICHALCZYK*, MAREK GAJOWY*

OPERATIONAL PROPERTIES OF VIBRATORY CONVEYORS OF THE ANTIRESONANCE TYPE

**WŁAŚCIWOŚCI EKSPLOATACYJNE PRZENOŚNIKA WIBRACYJNEGO
TYPU ANTYREZONANSOWEGO**

The hereby paper is devoted to the analysis of operational properties of vibratory conveyors, which principle of operations is based on the Frahm's dynamic elimination effect (Den Hartog, 1971). These conveyors, according to the data given by their producers have several advantages, among others, higher vibrations amplitudes at the same drive and exceptionally low dynamic forces transmitted to the foundation. The simulation model of such conveyor loaded with a feed was created in this work and investigations of the transport efficiency and forces transmitted to the foundation at stationary states as well as at start up and coasting periods were performed. Analytical tests of vibrations during unsteady motion periods were also performed and the method of determining maximum amplitudes of conveyors in the transient resonance during coasting was proposed. The research results indicate the possibility of a wide application of this type of machines in loose materials handling in various industry branches.

Keywords: antiresonant vibratory conveyor

W pracy zbudowano model matematyczny i symulacyjny nowego typu przenośnika wibracyjnego, którego schemat dynamiczny jest oparty na zasadzie działania eliminatora dynamicznego Frahma. Przenośniki takie są obecnie dostępne w handlu i według producentów posiadają szereg zalet, m.inn. możliwość zastosowania mniejszych jednostek napędowych i znikome przekazywanie drgań na podłoże. W pracy przeprowadzono badania symulacyjne podstawowych właściwości eksploatacyjnych tych maszyn przy różnym obciążeniu nadawą, przy czym w modelu uwzględniono wpływ nadawy sypkiej na ruch maszyny i bieg wibratorów napędowych i ich synchronizację.

Słowa kluczowe: antyrezonansowy przenośnik wibracyjny

---

*   AGH UNIVERSITY OF SCIENCE AND TECHNOLOGY, FACULTY OF MECHANICAL ENGINEERING AND ROBOTICS, AL. A. MICKIEWICZA 30,30-059 KRAKOW, POLAND

\#   Corresponding author: michalcz@agh.edu.pl

1. Introduction

Vibratory conveyors have several properties suitable in using them for materials handling in various industry branches. Among such properties the following can be mentioned: the resistance to high temperatures (of the order of 1000°C), possibility of heat acceptance from the transported material, possibility of transporting materials which are emitting poisonous gases and dusts, possibility of cooling and heating of feed materials and performing chemical reactions, etc.

New structures, which dynamic scheme is based on the dynamic elimination effect (Fig. 1) called (according to (Jiao, 2012)) antiresonance conveyors, are presently very popular in the vibratory conveyors market.
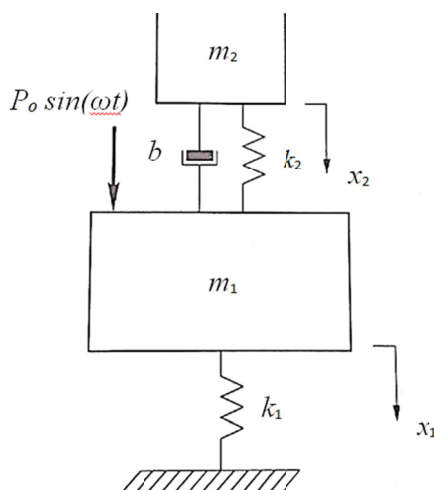
Fig. 1. Scheme of operation of antiresonance vibratory conveyors

Where:

m_1 — conveyor body mass,
m_2 — conveyor trough mass,
$P_0\sin(\omega t)$ — excitation force of the set of vibrators,
$k_{1,2}$ — coefficients of elasticity of suspensions,
$x_{1,2}$ — mass displacements in the motion direction, respectively.

The dynamic damper theory (Den Hartog, 1971) indicates that in case when the spring k_2 – on which mass m_2 is assembled – is tuned in such way as to have a partial frequency ω_2, being the natural vibrations frequency of mass m_2 on spring k_2, equal to the excitation frequency (1):

$$\omega = \omega_2 = \sqrt{\frac{k_2}{m_2}} \tag{1}$$

the amplitude of mass m_1 vibrations, in the steady state of the system without damping, is zeroing. This leads to the zero value of dynamic forces transmitted to the foundation.

Thus, this feature constitutes an advantage of this solution over classic structures. In addition, in the described structure, the mass of vibrators does not increase the vibrating mass, which allows to achieve – by means of the same vibrators – higher amplitudes of the vibrations of the trough, while the drive engines and elements of body supports are related – in the steady state – to an immobile mass which prolongs their service life. The idea of operations in the antiresonance state is used currently in constructing other vibratory machines, as e.g. vibrating screens shown in Fig. 2.

Fig. 2. Antiresonance screen of the VDL Industrial Process Company

Apart from patents of conveyors structures based on the Frahm's eliminator, e.g. (Long, 1960; Carmichael, 1982) there are only a few works considering dynamics of these machines, e.g. (Jiao, 2012; Liu, 2006; Czubak, 2012). Especially there is a lack of works investigating behaviour of this type of machines when their feed load is changing, or these works contain errors such as e.g. (Liu, 2012), which was indicated in (Czubak, 2013).

2. Aim of the work

The aim of this investigation was creating the dynamic model of the system, with taking into account the feed layered model, allowing to determine the transport efficiency dependence on a trough load as well as the dependence of the unit power and forces transmitted to the foundation on a trough load.

3. Vibratory conveyor model

The assumed a discrete dynamic scheme of the conveyor, with 6 degrees of freedom (x, y, α, f, φ_1, φ_2) for machine and with 24 degrees of freedom for 3-column and 4-layered feed is shown

304

in Fig. 3. The correctness of the theoretical principles of building calculation models of the machine body and the feed was based on experimental verification (Czubak & Michalczyk, 2001).
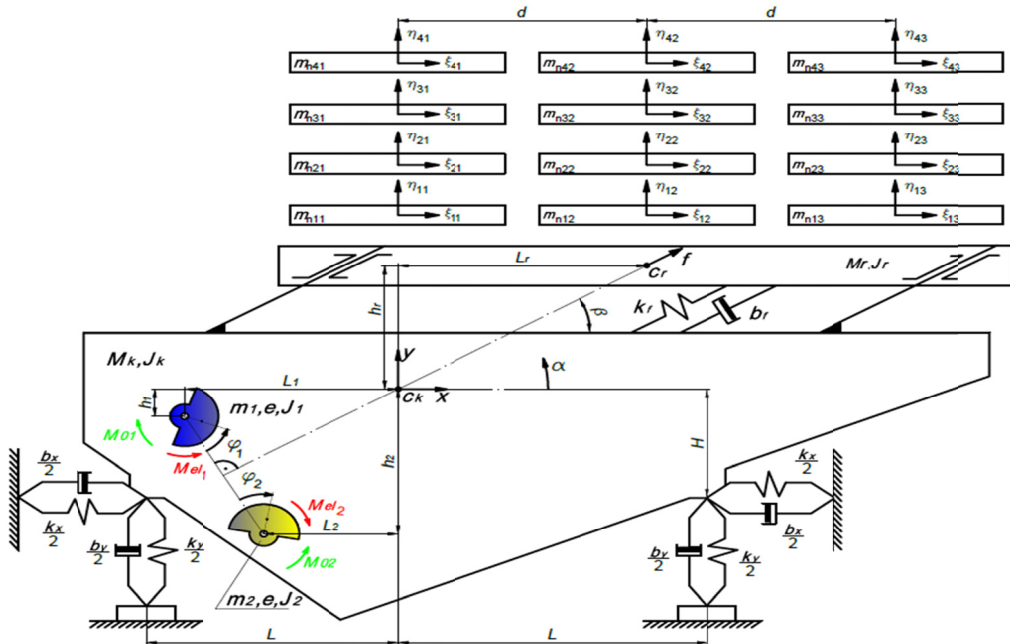
Fig. 3. Model of the vibratory conveyor, where f – relative displacement M_r in relation to M_k

The following constant values were assumed in simulations:
$L = 2$ m, $H = 0.48$ m, $l = 3d = 8$ m – the length of gutter,
$L_1 = 0.97$ m, $h_1 = 0.33$ m, $L_2 = 0.77$ m, $h_2 = 0.67$ m, $h_r = 1.1$ m, $L_r = 1.92$ m,

$k_x = k_y = 2328000$ N/m, $k_f = 10962000$ N/m – coefficients of elasticity,

$\psi_1 = 0.13$, $\psi_2 = 0.4$, $\psi_i = \dfrac{energy\ dissipated\ per\ cycle}{\max energy\ stored\ per\ cycle}$,

$b_x = \dfrac{\psi_1 k_x}{2\pi\omega}$, $b_y = \dfrac{\psi_1 k_y}{2\pi\omega}$, $b_f = \dfrac{\psi_2 k_f}{2\pi\omega}$ – coefficients of viscous damping

$m_{1.2} = 50$ kg, $M_r = 1000$ kg, $M_k = 2500$ kg – unbalanced mass of the vibrator, of the trough and body, respectively,
$m_n = 12 - 2000$ kg – total feed mass (variable),
$J_k = 12200$ kgm^2, $J_r = 5000$ kgm^2, $J_1 = J_2 = 0.18$ kgm^2 – central moments of inertia of the body, trough and rotating mass of the electrovibrator, respectively,
$e = 0.06$ m – radius of a vibrator unbalance,
$R_t = 0.005$ – coefficient of restitution of collisions between the first layer of the feed and the trough,

$R = 0.01$ – coefficient of restitution of collisions between successive layers of the feed,
$\mu_{tn} = 0.4$ – coefficient of friction between the first layer of the feed and the trough,
$\mu_{nn} = 0.7$ – coefficient of internal friction of the feed,

$P = 4$ kW – asynchronous engine power,
$M_{st} = 97.4$ Nm – stalling torque of the drive engine,
$\omega_s = 104.7$ rad/s, $\omega_{st} = 79.6$ rad/s – angular velocity of the synchronous running and of the stall, respectively.

The set of equations describing the machine motion can be written in a form:

$$\mathbf{M} \cdot \ddot{\mathbf{q}} = \mathbf{Q} \tag{2}$$

where:

$$\ddot{\mathbf{q}} = \frac{d^2}{dt^2}\begin{bmatrix} x & y & \alpha & f & \varphi_1 & \varphi_2 \end{bmatrix}^T \tag{3}$$

$$\mathbf{M} = \begin{bmatrix} m_1+m_2+M_k+M_r & 0 & h_1 m_1+h_2 m_2-h_r M_r & M_r\cos(\beta) & m_1\cos(\beta+\varphi_1)e & m_2\cos(\beta-\varphi_2)e \\ 0 & m_1+m_2+M_k+M_r & -L_1 m_1-L_2 m_2+L_r M_r & M_r\sin(\beta) & m_1\sin(\beta+\varphi_1)e & m_2\sin(\beta-\varphi_2)e \\ - & - & \begin{aligned}&J_k+J_r+L_1^2 m_1+\\&+L_2^2 m_2+L_r^2 M_r+h_1^2 m_1+\\&+h_2^2 m_2+h_r^2 M_r\end{aligned} & \begin{aligned}&L_r M_r\sin(\beta)+\\&-h_r M_r\cos(\beta)\end{aligned} & \begin{aligned}&-L_1 m_1\sin(\beta+\varphi_1)e+\\&+h_1 m_1\cos(\beta+\varphi_1)e\end{aligned} & \begin{aligned}&-L_2 m_2\sin(\beta-\varphi_2)e+\\&+h_2 m_2\cos(\beta-\varphi_2)e\end{aligned} \\ - & - & - & M_r & 0 & 0 \\ - & - & - & - & J_1+m_1 e^2 & 0 \\ - & - & - & - & - & J_2+m_2 e^2 \end{bmatrix} \tag{4}$$

$$\mathbf{Q} = \begin{bmatrix} \begin{aligned}&m_1\sin(\beta+\varphi_1)\dot{\varphi}_1^2 e - m_2\sin(\beta-\varphi_2)\dot{\varphi}_2^2 e+\\&-k_x(x+H\alpha)-b_x(\dot{x}+H\dot{\alpha})-T_{1(01)}-T_{1(02)}-T_{1(03)}\end{aligned} \\[2ex] \begin{aligned}&m_2\cos(\beta-\varphi_2)\dot{\varphi}_2^2 e - m_1\cos(\beta+\varphi_1)\dot{\varphi}_1^2 e+\\&-k_y y - \frac{b_y(\dot{y}-L\dot{\alpha})}{2} - \frac{b_y(\dot{y}+L\dot{\alpha})}{2} - F_{1(01)}-F_{1(02)}-F_{1(03)}\end{aligned} \\[2ex] \begin{aligned}&L_1 m_1\cos(\beta+\varphi_1)e\dot{\varphi}_1^2 - h_2 m_2\sin(\beta-\varphi_2)e\dot{\varphi}_2^2 - L_2 m_2\dot{\varphi}_2^2\cos(\beta-\varphi_2)e+\\&+h_1 m_1\sin(\beta+\varphi_1)e\dot{\varphi}_1^2 - b_x(\dot{x}+H\dot{\alpha})H - \frac{b_y(\dot{y}+L\dot{\alpha})L}{2}+\frac{b_y(\dot{y}-L\dot{\alpha})L}{2}+\\&-k_x(x+H\alpha)H - \frac{k_y(y+L\alpha)L}{2}+\frac{k_y(y-L\alpha)L}{2}+\\&+T_{1(01)}h_r + T_{1(02)}h_r + T_{1(03)}h_r - F_{1(02)}d - F_{1(03)}2d\end{aligned} \\[2ex] -b_f\dot{f}-k_f f \\[2ex] -gm_1\sin(\beta+\varphi_1)e + M_{el1} + M_{01} \\[2ex] -gm_2\sin(\beta-\varphi_2)e + M_{el2} + M_{02} \end{bmatrix} \tag{5}$$

The feed model was created on the basis of (Michalczyk, 2008):

$$F_{j,(j-1,k)} = (\eta_{j-1,k} - \eta_{j,k})^p k \left\{ 1 - \frac{1-R^2}{2} \left[\frac{1-\text{sgn}(\eta_{j-1,k} - \eta_{j,k})}{\text{sgn}(\dot{\eta}_{j-1,k} - \dot{\eta}_{j,k})} \right] \right\} \tag{6}$$

$$T_{j,(j-1,k)} = -\mu F_{j,(j-1,k)} \, \text{sgn}(\dot{\xi}_{j,k} - \dot{\xi}_{j-1,k}) \tag{7}$$

$F_{j,(j-1,k)}$ — normal component of the j-th layer pressure on the $j-1$ layer in the k-th column,
$T_{j,(j-1,k)}$ — tangent component of the j-th layer pressure on the $j-1$ in the k-th column, being the friction force.

When the successive feed layers: j-th and $j-1$ (in the given column) are not in contact, the pressure force between these layers in the normal $F_{j,(j-1,k)}$ and tangent direction $T_{j,(j-1,k)}$ is equal zero. Equations of motion in x and y directions of individual feed layers, with taking into account the conveyor influence on lower feed layers, are of a form:

$$m_{nj,k}\ddot{\xi} = T_{j,(j-1,k)} - T_{j+1,(j,k)} \tag{8}$$

$$m_{nj,k}\ddot{\eta} = -m_{nj,k}g + F_{j,(j-1,k)} - F_{j+1,(j,k)} \tag{9}$$

4. Analysis of steady states – simulation results

4.1. Conveyor not loaded with a feed – the process of vibrations steadying after the machine was switched on
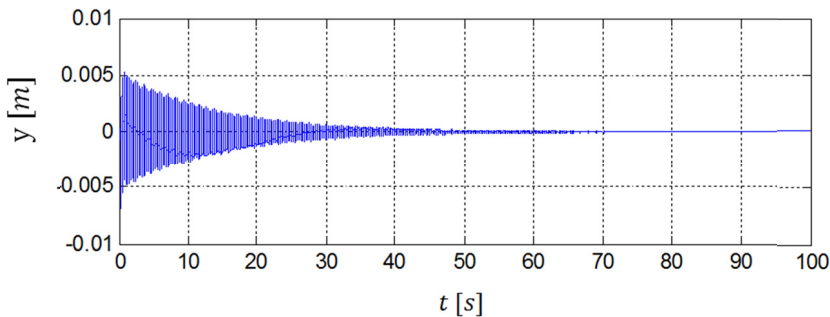
Fig. 4. Vertical displacement of the conveyor body mass as a time function
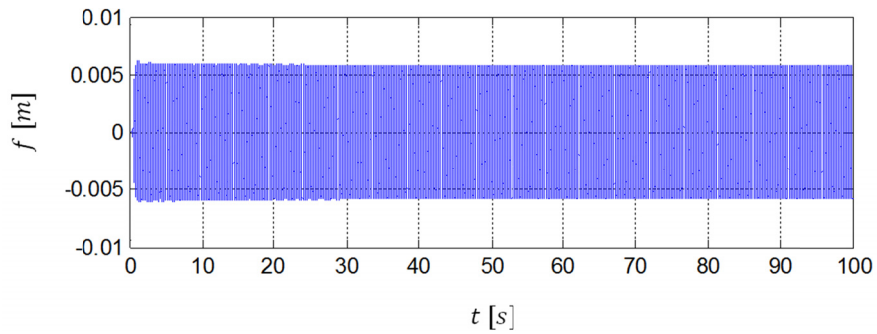
Fig. 5. Displacement of the trough f versus the body as a time function
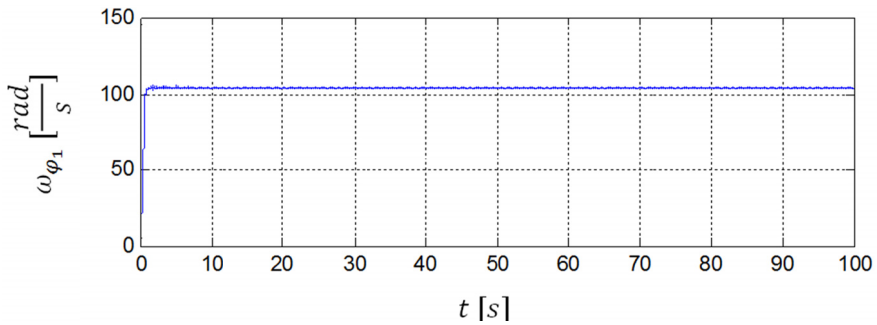
Fig. 6. Angular velocity of the vibrator 1 as a time function
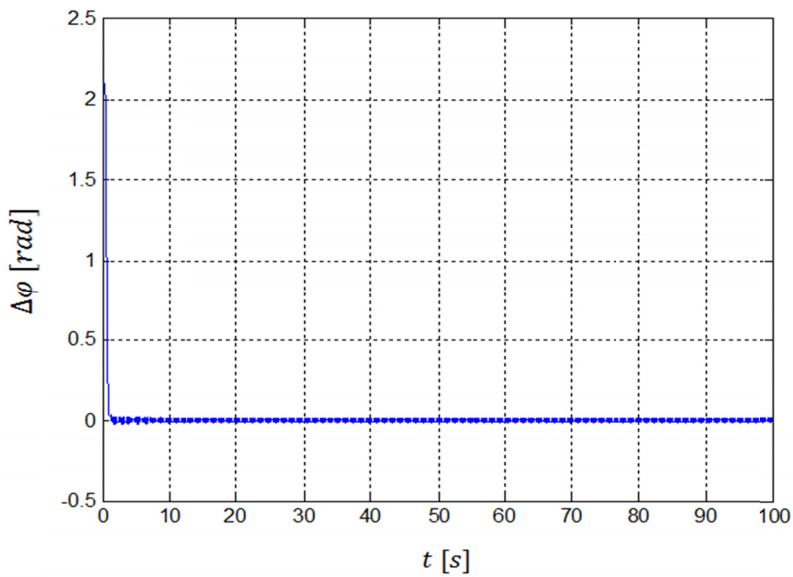
Fig. 7. Difference of angular displacements $\Delta\varphi$ of vibrators 1 and 2 as a time function

4.2. Conveyor loaded with a feed of a total mass of 840 kg – the process of vibrations steadying after the machine was switched on
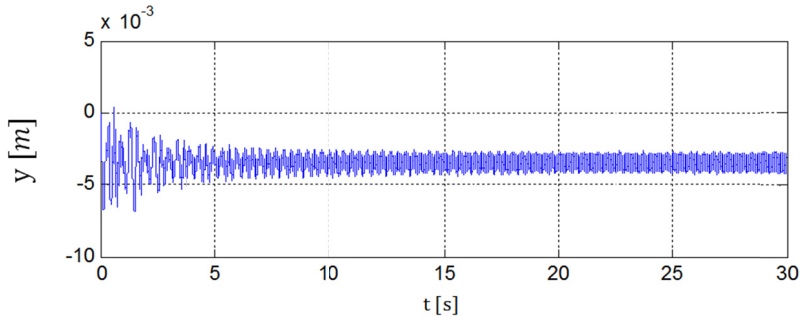
Fig. 8. Vertical displacement y as a time function
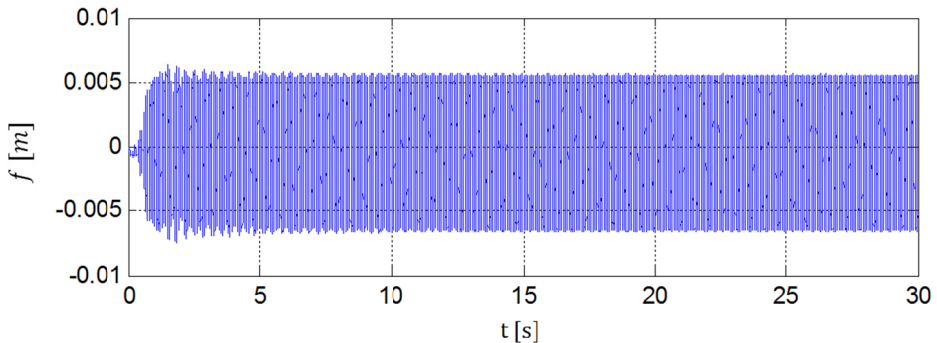
Fig. 9. Relative displacement f of the trough versus the body, as a time function

Comparison of Fig. 4. and Fig. 8. indicates a significant influence of the feed on limiting the transient resonance and on increasing the amplitudes of vertical vibrations in the steady state.

4.3. Feed velocity as a function of the feed amount on the conveyor

These findings confirm the results achieved in papers: (Czubak, 2007, 2012), where it was proved that regardless of loading the conveyor with a significant feed amount, at the properly selected (of a value app. 3) coefficient of throw (ratio of amplitude of vertical component of acceleration of the trough to the gravitational acceleration), the conveyor still maintains high transport velocities.
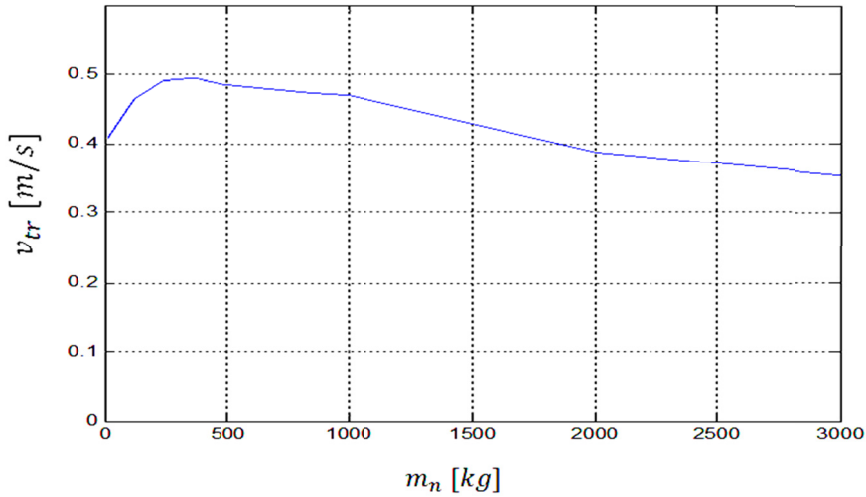
Fig. 10. Dependence of the average transport velocity v_{tr} (averaged in layers) of the conveyor loaded with the feed m_n

4.4. Efficiency as the feed amount function

The function allowing to determine the conveyor efficiency, in dependence of the feed amount being on the conveyor and the average transport velocity, is of a form:

$$Q = \frac{m_n}{l} v_{tr}, \quad \left[\frac{\text{kg}}{\text{s}} \right] \tag{10}$$

where: Q — efficiency, m_n — mass of the feed being on the conveyor trough, l — length of the trough, v_{tr} — average transport velocity.

As can be seen from the diagrams of Fig. 10.11, in the examined range, along with the increase in the amount of feed on the conveyor, the efficiency gets bigger, while this increase decreases with the increase in the weight of the feed.

4.5. Maximum dynamic force transmitted to the foundation as the efficiency function

Maximum dynamic force transmitted to the foundation as the function of efficiency Fig. 12, was obtained on the basis of numerical simulation of conveyor's vibrations and the formula (11).

The method of calculating the average value of the foundation load at the steady state:

$$R_{\max} = \sqrt{(\Sigma R_x)^2 + (\Sigma R_y)^2}, \quad [\text{N}] \tag{11}$$

where:

ΣR_x — total dynamic force acting on the supporting springs in direction x,
ΣR_y — total dynamic force acting on the supporting springs in direction y.

310
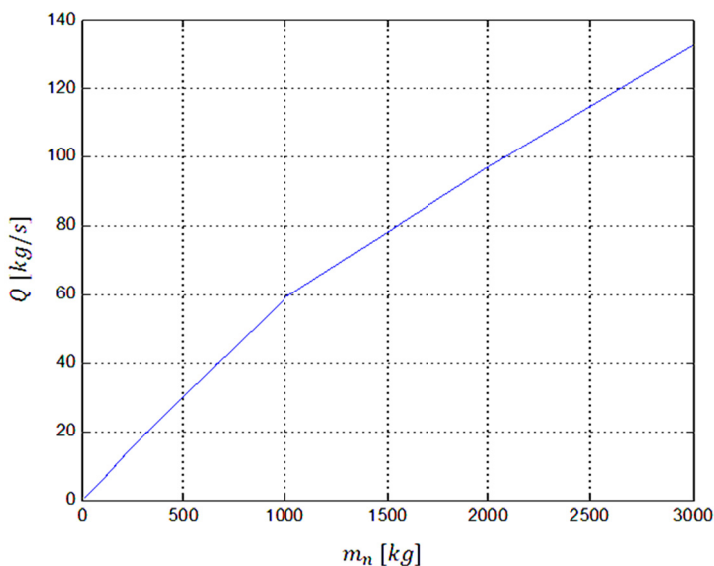
Fig. 11. Conveyor efficiency Q as a function of the feed mass being on the conveyor trough m_n
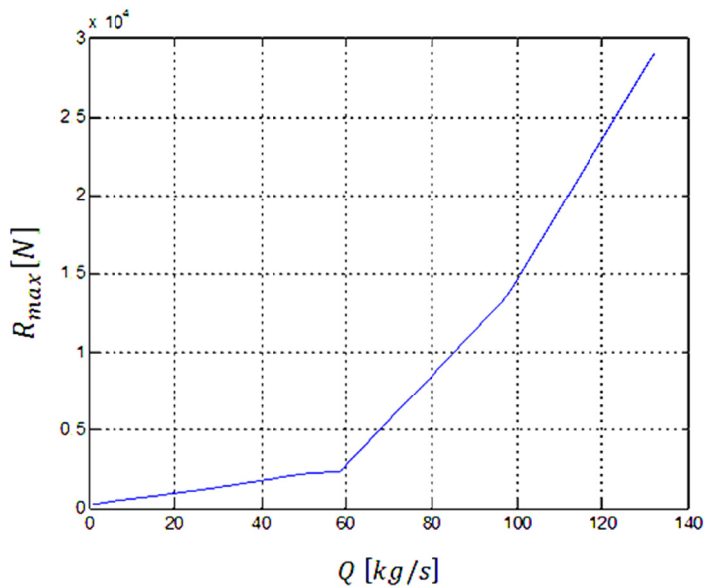
Fig. 12. Maximum force transmitted to the foundation as the efficiency function

As can be seen from the graph Fig. 12, the vibrator synchronization gets disturbed during the conveying process (Gajowy, 2018) and it causes the increase of vibrations of the body and forces transmitted to the foundation.

4.6. Ratio of the power demand to the efficiency as the efficiency function
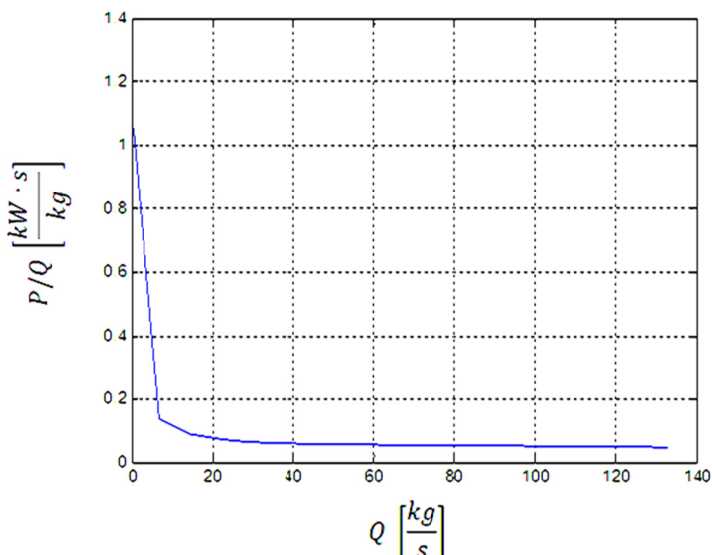
Fig. 13. Ratio of the power demand to the efficiency as the efficiency function obtained
on the basis of simulation

The graph in Fig. 13 shows that the energy consumption for transporting the unit amount of feed is decreasing with the increase of efficiency. Transport becomes the most cost-effective if the efficiency exceeds $Q = 25$ kg/s. Maximum efficiency was not specified in the work. However, it has limitations due to the dynamic load on the ground and strength parameters of the gutter and the whole conveyor and it is associated with the appropriate selection of the drive power.

5. Analysis of non-stationary states

The conveyor behaviour during the transient resonance at start-up and coasting is important from the point of view of technological applications. That time multiple increases of vibration amplitudes can lead to machine damages or to an excessive loading of the supporting structure. Since the start-up is rather fast, a higher threat is related to the vibrator free coasting after the engine switching-off. In order to investigate this problem for the case of antiresonance conveyor the frequencies and forms of its natural frequencies should be determined.

5.1. Analysis of natural frequencies and forms of vibrations

Due to a small energy scattering in springs – originated mainly from material and structural damping – it is possible to analyse natural vibrations of the system as undamped vibrations. Re-

maining non-linearities of the machine model, without a feed, are related to the influence of body vibrations on the vibrators motion and with the Coriolis acceleration in the trough complex motion. Dimension to mass ratios – in typical structures of vibratory machines – generally allow to omit, in the analysis, motion of the vibrator and its mass concentration in the axis of rotation (Blechman, 1994). In a similar fashion, when analysing the Coriolis acceleration values, it is possible to omit them – for typical dimensional relations of the machine – in comparison to the remaining acceleration components. Thus, it is possible to reduce dynamic equations (2) to (5) to a form:

$$\mathbf{M} \cdot \ddot{\mathbf{q}} + \mathbf{K} \cdot \mathbf{q} = \mathbf{0} \tag{12}$$

where: $\mathbf{0}$ — zero value, $\mathbf{M}$ — mass matrix, $\mathbf{K}$ — elasticity matrix.

The general solution of the homogeneous equation assumes a form:

$$\mathbf{q} = \mathbf{q_o} \sin(\omega t + \gamma) \tag{13}$$

where: $\mathbf{q_o}$ — vector of coordinates amplitudes: $x, y, \alpha, f,$ ω — natural frequency, γ — phase angle of vibrations.

From that the matrix equation is obtained :

$$(\mathbf{K} - \omega^2 \cdot \mathbf{M}) \cdot \mathbf{q} = \mathbf{0} \tag{14}$$

When the matrix: $(\mathbf{K} - \omega^2 \cdot \mathbf{M})$ is a singular one, i.e.

$$\det(\mathbf{K} - \omega^2 \cdot \mathbf{M}) = 0 \tag{15}$$

there is a possibility of non-zero solution of this equation.

The above dependence constitutes the 4-th degree equation for ω^2 and leads to determining 4 natural frequencies (not necessary different). Frequencies – ω are rejected, since they are without any physical sense. After taking into account forms of mass and elasticity matrices, the left member of the equation assumes a form:

$$\left(\mathbf{K} - \omega^2 \cdot \mathbf{M}\right) = \begin{bmatrix} k_x - (M_k + M_r)\omega^2 & 0 & k_x H + h_r M_r \omega^2 & -M_r \cos(\beta)\omega^2 \\ 0 & k_y - (M_k + M_r)\omega^2 & -L_r M_r \omega^2 & -M_r \sin(\beta)\omega^2 \\ k_x H + h_r M_r \omega^2 & -L_r M_r \omega^2 & k_x H^2 + k_y L^2 + \\ -\begin{bmatrix} J_k + J_r + \\ + M_r L_r^2 + M_r h_r^2 \end{bmatrix}\omega^2 & \begin{bmatrix} -M_r L_r \sin(\beta) + \\ + M_r h_r \cos(\beta) \end{bmatrix}\omega^2 \\ -M_r \cos(\beta)\omega^2 & -M_r \sin(\beta)\omega^2 & \begin{bmatrix} -M_r L_r \sin(\beta) + \\ + M_r h_r \cos(\beta) \end{bmatrix}\omega^2 & -M_r \omega^2 + k_s \end{bmatrix} \tag{16}$$

After substituting the previously assumed numerical values, the solution in the form of 4 natural frequencies is obtained:

$\omega_1 = 18.4$ rad/s,
$\omega_2 = 25.6$ rad/s,
$\omega_3 = 29.6$ rad/s,
$\omega_4 = 125$ rad/s.

Since zeroing of the main matrix determinant means that equations are linearly dependent, it is not possible to obtain exact values of amplitudes. Substituting – into the matrix – the given natural frequency will allow to determine **forms of vibrations**, it means ratios of amplitudes of individual coordinates.

The following forms of vibrations were obtained for exact frequency values:

$$\mathbf{q_o} = \begin{pmatrix} A \\ B \\ C \\ D \end{pmatrix} \tag{17}$$

Calculation of the first form of vibrations for $\omega_1 = 18.427$ rad/s

$$\left(\mathbf{K} - \omega^2 \cdot \mathbf{M}\right) \cdot \mathbf{q_o} = \begin{bmatrix} 1.14 \cdot 10^6 & 0 & 1.494 \cdot 10^6 & -2.941 \cdot 10^5 \\ 0 & 1.14 \cdot 10^6 & -6.519 \cdot 10^5 & -1.698 \cdot 10^5 \\ 1.494 \cdot 10^6 & -6.519 \cdot 10^5 & 2.339 \cdot 10^6 & 0 \\ -2.941 \cdot 10^5 & -1.698 \cdot 10^5 & 0 & 1.062 \cdot 10^7 \end{bmatrix} \cdot \begin{pmatrix} A \\ B \\ C \\ D \end{pmatrix} = \begin{pmatrix} 0 \\ 0 \\ 0 \\ 0 \end{pmatrix} \tag{18}$$

Using the matrix distribution LU the vibration form referred to the relative displacement amplitude f was obtained:
- for $\omega_1 = 18.4$ rad/s,

$$\begin{pmatrix} A \\ B \\ C \\ D \end{pmatrix} = \begin{pmatrix} 48.07 \\ -20.71 \\ -36.47 \\ 1 \end{pmatrix} \cdot D \tag{19a}$$

- for $\omega_2 = 25.6$ rad/s,

$$\begin{pmatrix} A \\ B \\ C \\ D \end{pmatrix} = \begin{pmatrix} 9.98 \\ 14.17 \\ 0.12 \\ 1 \end{pmatrix} \cdot D \tag{19b}$$

- for $\omega_3 = 29.6$ rad/s,

$$\begin{pmatrix} A \\ B \\ C \\ D \end{pmatrix} = \begin{pmatrix} 26.35 \\ -22.68 \\ 9.76 \\ 1 \end{pmatrix} \cdot D \tag{19c}$$

- for $\omega_4 = 125$ rad/s,

$$\begin{pmatrix} A \\ B \\ C \\ D \end{pmatrix} = \begin{pmatrix} -0.259 \\ -0.149 \\ -0.000924 \\ 1 \end{pmatrix} \cdot D \qquad (19d)$$

Determining the amplitude at coasting by means of the energy balance method

Due to a loss of a cophasal running of vibrators occurring in the circum-resonant range of the system (Fig. 14), other methods of assessing maximum amplitudes in the transient resonance cannot be applied (Cieplok, 2009), since they assume the cophasal running of vibrators and without such running they do not allow to determine the maximum amplitudes of angular vibrations of the machine.
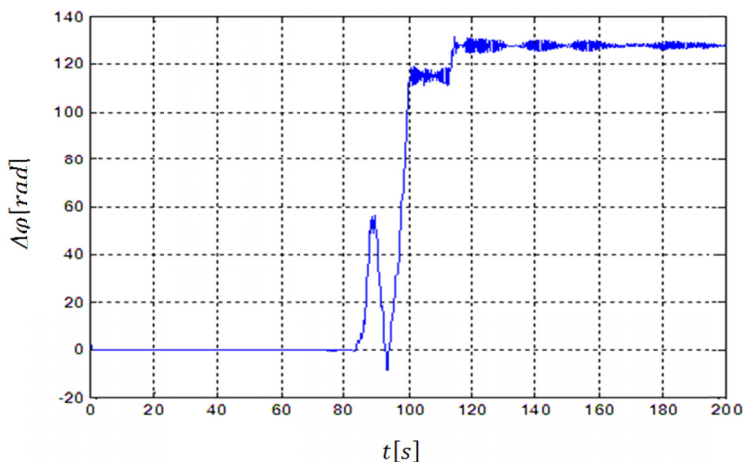
Fig. 14. Difference of angular displacements of engines 1 and 2 at coasting

Therefore the energy balance method was applied for the analysis of maximum amplitudes (Michalczyk, 2012).

This method is based on the assumption that the energy of the set of vibrators, with which they enter the transient resonance, is mainly transformed into the body vibration energy increase. This effect causes an abrupt decrease of the vibrators angular frequency within the circum-resonant range, shown in Fig. 15.

Thus, the energy balance is as follows:

$$n\frac{1}{2}J_{zr}\omega_{0i}^2 = \frac{1}{2}\dot{\mathbf{q}}_{\mathbf{maxi}}^{\mathbf{T}}\mathbf{M}\dot{\mathbf{q}}_{\mathbf{maxi}} \qquad (20)$$

where:

n — number of vibrators,

J_{zr} — moment of inertia of the drive system reduced to the rotor shaft,
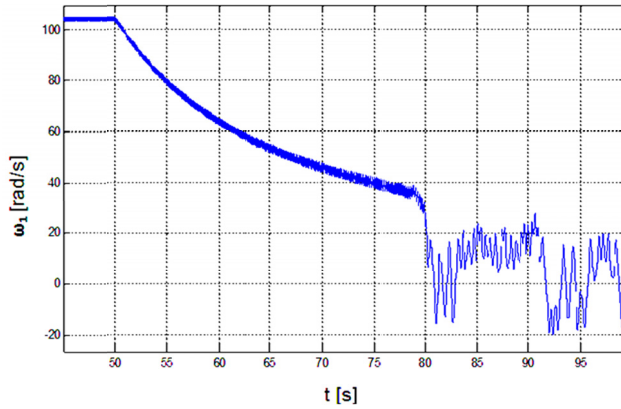
Fig. 15. Effect of loosing the vibrator angular frequency in the circum-resonant range

ω_{0i} — angular velocity at which the energy transfer occurs (in approximation: the i-th natural frequency of the system),

$\mathbf{q_{max\,i}}$ — coordinates vector describing vibrations of the system with the i-th vibration form,

$\mathbf{M}$ — mass matrix of the linearised vibrating system, determined on the basis of (21).

The kinetic energy of the body for small vibrations, near the balance point is of the approximate form:

$$E_{kin\_k} = \frac{1}{2}J_k\dot{\alpha}^2 + \frac{1}{2}J_r\dot{\alpha}^2 + \frac{1}{2}\begin{bmatrix}(\dot{y}+L_r\dot{\alpha}+\dot{f}\sin(\beta))^2 + \\ +(\dot{x}-h_r\dot{\alpha}+\dot{f}\cos(\beta))^2\end{bmatrix}\cdot m_r + \frac{1}{2}\left[\dot{y}^2+\dot{x}^2\right]\cdot m_k \qquad (21)$$

which allows to determine the mass matrix $\mathbf{M}$ (22).

$$\mathbf{M} = \begin{bmatrix} M_k+M_r & 0 & -h_rM_r & M_r\cos\beta \\ 0 & M_k+M_r & L_rM_r & M_r\sin\beta \\ -h_rM_r & L_rM_r & J_k+J_r+M_rL_r^2+M_rh_r^2 & M_rL_r\sin\beta-M_rh_r\cos\beta \\ M_r\cos\beta & M_r\sin\beta & M_rL_r\sin\beta-M_rh_r\cos\beta & M_r \end{bmatrix} \qquad (22)$$

For harmonic vibrations of frequency ω_{0i} the vector of maximum velocities is related to the vector of maximum amplitudes of displacements by the following dependency:

$$\dot{\mathbf{q}}_{\mathbf{max\,i}} = \omega_{0i}\,\mathbf{q_{max\,i}} \qquad (23)$$

After substituting (22) into (20) and the reduction:

$$nJ_{zr} = \mathbf{q_{max\,i}^T}\,\mathbf{M}\,\mathbf{q_{max\,i}} \qquad (24)$$

For each i-th natural frequency we know the modal vector (19a-d) allowing to determine the dependence between vibration amplitudes, i.e. vibration forms:

$$\mathbf{\Psi_i}(\omega_i) = col\{A_i, B_i, C_i, D_i\}$$

Thus, the vector determining the vibration amplitudes in the *i*-th resonance can be presented e.g. as below:

$$\mathbf{q_{maxi}} = col\left\{\frac{A_i}{D_i}D_i, \frac{B_i}{D_i}D_i, \frac{C_i}{D_i}D_i, D_i\right\} = D_i col\left\{\frac{A_i}{D_i}, \frac{B_i}{D_i}, \frac{C_i}{D_i}, 1\right\} = D_i\mathbf{a_i} \tag{25}$$

where: D_i is the maximum amplitude of coordinate *f*, while $\mathbf{a_i}$ is the vector of ratios of amplitudes of the system coordinates *x*, *y*, *α* to the coordinate amplitude *f* during the *i*-th resonance.

After introducing the above dependencies into the energy balance we finally obtain the equation for the maximum coordinate amplitude *f* when the system is passing through the resonance with the *i*-th vibration frequency:

$$D_i = \sqrt{\frac{nJ_{zr}}{\mathbf{a_i^T M a_i}}} \tag{26}$$

The remaining amplitudes A_i, B_i, C_i in the *i*-th resonance can be determined knowing their ratio to D_i (from 19a,b,c,d).

The maximum amplitudes of vibrations determined in this way in successive resonances are listed in Table 1.

For comparing reasons, values of maximum amplitudes obtained by means of numerical simulations of the model formulated in item 3, without differentiation which resonance they concern, are also placed in this Table. Due to a vicinity of successive resonances such differentiation is not possible (Fig. 16).

The calculation error was determined as a difference between maximum values out of successive resonances obtained by means of the energy balance method and maximum values for the whole coasting process obtained by means of the simulation.

TABLE 1

Vibration amplitudes at coasting with using the energy balance (Michalczyk, 2012) with individual resonance frequencies of vibrators (maximum amplitudes for the given degree of freedom are marked by a thickened font). The resonance amplitude was not determined for the coordinate *f,* because in relation to it the circum resonant amplification of vibrations does not occur – Fig. 16d, since the system is not passing through the resonance with the highest natural frequency $\omega_4 = 125$ rad/s

	$\omega_1 = 18.4$ rad/s	$\omega_2 = 25.6$ rad/s	$\omega_3 = 29.6$ rad/s	Simulation	Relative error
x [m]	0.00426	0.00574	**0.00711**	**0.013**	45%
y [m]	−0.00184	**0.00815**	−0.00612	**0.012**	32%
α [rad]	**−0.00323**	0.000069	0.00264	**0.0038**	15.9%
f [m]	0.00009	0.000575	0.00027	—	—

A relatively low accuracy of the analytical method is caused by the fact that individual natural frequencies ω_1, ω_2, ω_3, through which the system is passing, are very close – one to another – and the method assumption concerning separate occurrences of successive resonances is not met (Michalczyk, 2012).
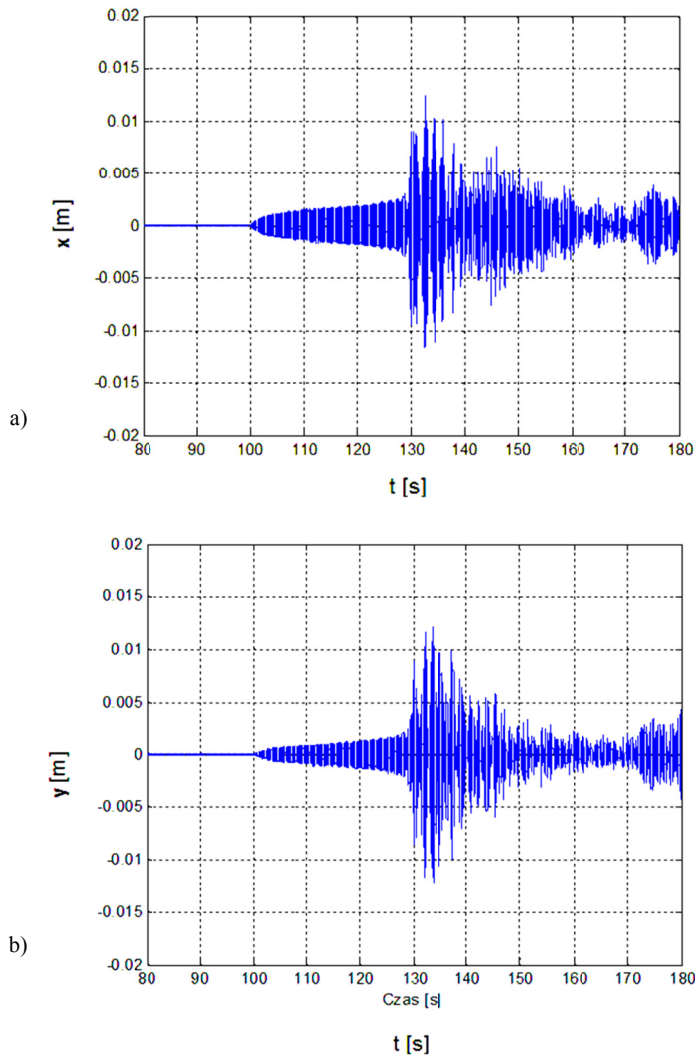
Fig. 16. Free coasting of the machine (the drive was switched off in the 100-th second of the simulation):
a) Horizontal displacement of the body, b) Vertical displacement of the body

6. Conclusions

Operational properties of antiresonance vibratory conveyors were analysed in the paper. The mathematical model of such conveyor was created taking into account a limited drive power, vibrators selfsynchronisation effect and the feed influence. Simulation investigations of the vibratory transport efficiency and dynamic forces transmitted to foundations as a function of the conveyor loading with a feed, were performed. Analytical tests of vibrations during unsteady motion periods were also performed and the method of determining maximum amplitudes of

c)

d)
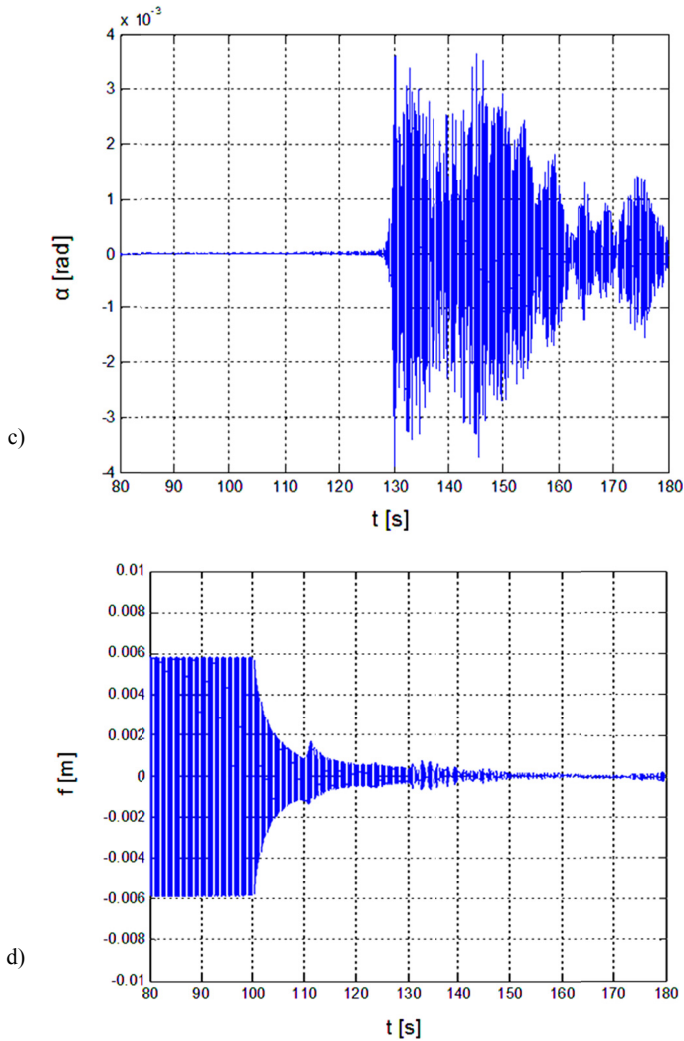
Fig. 16. Free coasting of the machine (the drive was switched off in the 100-th second of the simulation):
c) Angular displacement of the body, d) Relative displacement of the trough

conveyors in the transient resonance during coasting was proposed. Some other important findings are given below.

1°. Average transport velocity of the feed on the antiresonance conveyor, except for very small and very large (when the feed mass exceeds the trough mass) loads is a slowly decreasing function of the feed mass on the trough (Fig. 10). Thus, the antiresonance conveyor efficiency in this zone in a approximate linear fashion depends on the feed mass being on the trough (Fig. 11).

2°. Maximum dynamic force transmitted to the foundation is – in approximation – proportional to the actual conveyor efficiency (Fig. 12).

3°. The energy balance method (Michalczyk, 2012), as giving in this particulary case not very accurate results because of close vicinity of resonant frequencies, should be modified (Gajowy, 2018).

4°. On the bases of the performed investigations it can be stated that antiresonance conveyors constitute a favourable alternative for classic solutions, in case when there is a need of limiting dynamic forces transmitted to the foundation at the stationary state and at transient periods.

Acknowledgements

References

Blechman I.I., 1994. *Wibracjonnaja Mechanika.* Nauka, Moskwa.

Carmichael D., 1982. *Excited Frame Vibratory Conveying Apparatus for Moving Particle Material.* US Patent 4 313 535.

Cieplok G., 2009. *Stany nieustalone nadrezonansowych maszyn wibracyjnych.* Wyd. AGH, Kraków.

Czubak A., Michalczyk J., 2001. *Teoria transportu wibracyjnego.* Wyd. Pol. Świetokrzyskiej, Kielce.

Czubak P., Michalczyk J., 2007. *Własności ruchowe przenośników wibracyjnych działających na zasadzie eliminatora dynamicznego.* Modelowanie Inżynierskie **2**, 33, 55-61. ISSN 1896-771X, Gliwice.

Czubak P., 2012. *Reduction of forces transmitted to the foundation by the conveyor or feeder operating on the basis of the Frahm's eliminator, at a significant loading with feed.* Archives of Mining Sciences **57**, 4.

Czubak P., 2013. *Wybrane zagadnienia dynamiki przenośników wibracyjnych.* Wyd. AGH, Kraków.

Den Hartog J.P., 1971. *Drgania mechaniczne.* PWN, Warszawa.

Gajowy M., 2018. *Rozprawa doktorska na Wydziale IMiR AGH.* Kraków.

Jiao C., Liu J., Wang Q., 2012. *Dynamic Analysis of Nonlinear Antiresonant Vibration Machine Based on General Finite Element Method.* Advanced Material Research **443**.

Liu Jie, Liu Jintao, Xu H., 2006. *Dynamical Analysis and Control of Driving Point Anti-resonant Vibrating Machine Based on Amplitude Stability.* Chinese Journal of Mechanical Engineering **1**.

Liu Q., 2012. *The material of the resonant vibration impact motivates the influence of and the simulation analysis.* Advanced Material Research **510**.

Long G., Tsuchiya T.,1960. *Vibratory conveyors.* US Patent 2 951 581.

Michalczyk J., 2008. *Phenomenon of Force Impulse Restitution in Collision Modelling.* Journal of Theoretical and Applied Mechanics **46**, 4.

Michalczyk J., 2012. *Transient Resonance of Machines and Devices in General Motion.* Journal of Theoretical and Applied Mechanics **2**.

VDL Vibrating Conveyors:

http://www.vdlindustrialproducts.com/?page/3186532/Vibrating+conveyors.aspx